High-Propellant Throughput Sub-kW Electric Propulsion System for Deep Space Science and Exploration

IEPC-2022-343

Presented at the 37th International Electric Propulsion Conference
Massachusetts Institute of Technology, Cambridge, MA USA
June 19-23, 2022

Gabriel F. Benavides[1] , Hani Kamhawi[2], Timothy R. Sarver-Verhey[3], Corey R. Rhodes[4], Matthew J. Baird[5], and Jonathan A. Mackey[6]
NASA Glenn Research Center, Cleveland, Ohio, 44135, USA

The National Aeronautics and Space Administration (NASA) is maturing high-propellant throughput sub-kilowatt electric propulsion technologies to enable small spacecraft deep space science and exploration missions with high delta-v requirements. The pathfinder model (PM) propulsion system consists of the H71M-PM Hall-effect thruster, a breadboard 1-kW power processing unit (PPU), and a propellant flow control system. The propulsion system requirements balance the needs of various high delta-v NASA and commercial industry mission concepts to achieve a design that both enables a variety of NASA small spacecraft deep space missions, while remaining viable for select commercial applications. The H71M-PM thruster has completed performance characterization and three 500-h short duration wear tests (SDWT). The propulsion system provides stable thrust generation over a wide range of operating conditions from 200 W to 1 kW, and 200 V to 400 V. The thruster has demonstrated a thrust as high as 68 mN at 300 V and 1 kW. The thruster has similarly demonstrated a specific impulse of 1850 s at 400 V and 1 kW. Key surfaces were machined between each SDWT to simulate accelerated discharge channel and pole cover erosion. Profilometry scans across masked pole cover surfaces were conducted to determine erosion rates. SDWT results indicate that a target thruster lifetime of 14 kh with 50% margin is feasible, although further verification is needed. Component testing has demonstrated propellant azimuthal flow uniformity better than ± 2 percent of the nominal value, azimuthal magnetic field uniformity better than ± 0.5 percent of the nominal value, and cathode heater cycle testing to greater than 30,000 cycles. A second-generation breadboard PPU has been fabricated and is currently under test. Propulsion system integrated system testing is planned to use the H71M-PM and the breadboard 1-kW PPU. Pathfinder model test results are now supporting the design of the H71M-EM engineering model thruster. NASA has made these technologies available to U.S. industry through a no cost, nonexclusive licensing agreement.

I. Introduction

The National Aeronautics and Space Administration (NASA) regularly invests in new propulsion technologies that support a strategic goal [1] to increase the use of low-cost small spacecraft to conduct science and exploration missions. Decades of past NASA in-space propulsion investments have already supported the maturation of many chemical, cold-gas, and electric propulsion technologies presently enabling small spacecraft missions in low Earth

[1] Senior Research AST, Electric Propulsion System Branch, AIAA Senior Member, gabriel.f.benavides@nasa.gov.
[2] Senior Research AST, Electric Propulsion System Branch, AIAA Associate Fellow.
[3] Senior Research AST, Electric Propulsion System Branch, AIAA Senior Member.
[4] Research AST, Electric Propulsion System Branch, AIAA Member.
[5] Research AST, Electric Propulsion System Branch.
[6] Research AST, Electric Propulsion System Branch.

orbits (LEO) [2]. Some of these low power technologies have further proven extensible to certain deep space missions with modest propulsive requirements [3] [4]. However, a technology gap persists for high-propellant throughput sub-kW electric propulsion systems needed to support high delta-v NASA small spacecraft deep space science and exploration missions.

While the number of commercial sub-kW electric propulsion products has grown considerably in recent years [2], most of these systems have been optimized for the LEO market. The rapidly expanding use of small spacecraft in LEO offers suppliers a significant opportunity for sales volume and revenue, important considerations in developing a business case for a new propulsion product. In just the last five years, the number of small spacecraft deployed in LEO with electric propulsion systems has exceeded all prior years combined. While the growing application of electric over chemical propulsion is a paradigm shift for the spacecraft industry, certain facts remain unchanged. Commercial small spacecraft developers demand the absolute best price from propulsion system developers commensurate with their target spacecraft cost.

Minimizing costs typically implies matching propulsion system capability and reliability with the commercial mission minimum requirements. Given the large disparity in requirements between a typical commercial LEO and NASA deep space small spacecraft mission, the propulsion products gaining flight heritage in LEO are naturally inadequate for most NASA deep space missions. Higher performance, and consequently more expensive, electric propulsion products have matured far more slowly or been abandoned altogether due to poor commercial interest. While some commercial small spacecraft mission concepts could benefit from higher-performance propulsion products, the infrequency of such missions limits the business case for commercial electric propulsion developers. A key challenge for NASA is to identify and support higher delta-v commercial applications (with similar requirements to NASA deep space missions) that will sustain long-term commercial use of higher propellant throughput sub-kW electric propulsion, so NASA can be a marginal buyer.

This paper describes NASA's recent progress in the development of a high-propellant throughput sub-kilowatt Hall-effect propulsion system. This work builds upon the technologies reported in previous publications [5] [6]. The evolving system requirements, relative to prior publications, reflect the SSEP project's dedication to maturing system requirements that address higher delta-v commercial mission concepts, not presently supported by existing domestic commercial propulsion products, while simultaneously addressing NASA deep space mission needs.

II. Technology Development Philosophy

NASA's Small Spacecraft Electric Propulsion (SSEP) project seeks to address the lack of a sufficiently high performance and high-propellant throughput sub-kW electric propulsion product by maturing relevant electric propulsion technologies to a high technology readiness level (TRL) and then making the technologies available to U.S. industry through no cost, non-exclusive licensing agreements [7]. By making the necessary investments to raise the TRL of these higher-performance technologies, NASA minimizes otherwise prohibitive development costs for most small businesses. Furthermore, the SSEP project seeks U.S. industry input to establish synergy in propulsion system requirements between credible higher delta-v commercial and NASA mission concepts to maximize opportunity for domestic commercialization. While seeking such synergy inevitably means relaxing historic NASA propulsion system requirements, the SSEP project recognizes that striking the right balance between NASA and commercial requirements is a critical factor toward achieving a successful technology commercialization. As the technologies mature, the SSEP project will continue to seek synergy with commercial industry and transfer the technologies to credible U.S. entities for commercialization.

The SSEP project defines small spacecraft as robotic vehicles with a wet mass of roughly between 180 kg and 450 kg. The SSEP project does not specifically mature technologies for a subset of small spacecraft commonly referred to as CubeSats. The 180 kg wet mass is particularly relevant to NASA stakeholders, as is evident by the mass restrictions in recent Announcement of Opportunities (AO) [8]. Such mass restrictions are at least in part driven by the historic relationship between mission cost and spacecraft wet mass, where these low-cost NASA funded mission opportunities have cost caps theoretically consistent with a 180 kg mass limit. On the other hand, commercial missions are typically capability and revenue driven, which often result in spacecraft wet masses exceeding 180 kg. For commercial missions, the additional revenue generated by incremental increases in spacecraft size can exceed the additional launch cost, justifying mass growth. The SSEP project seeks to develop technologies and devices relevant to the full 180 kg to 450 kg small spacecraft wet mass range to equally support both NASA and commercial high delta-v mission needs.

The SSEP project currently focuses on sub-kW Hall-effect thruster technology given its good balance of thrust, thrust-to-power, and specific impulse. Furthermore, Hall-effect thrusters are relatively straightforward to fabricate compared to gridded-ion thrusters. Hall thrusters have extensive flight history and are generally well-understood

devices. The project seeks to advance systems, subsystems, components, and processes to further improve sub-kW Hall-effect propulsion system performance, lifetime, reliability, manufacturability, and cost. The project seeks to collectively optimize these parameters to best support NASA small spacecraft missions, while maintaining a feasible path toward becoming commercially sustainable. For example, performance and lifetime are optimized to enable future small spacecraft deep space missions, but not unnecessarily optimized at the expense of cost and manufacturability, which might undermine commercialization. Striking a good balance in requirements and design approach is achieved through regular communication and collaboration with NASA and U.S. industry stakeholders.

III. Sub-kW Electric Propulsion System Overview

The SSEP project is presently maturing a sub-kW electric propulsion system based on Hall-effect thruster technology. The system consists of a Hall-effect thruster, a 1-kW power processing unit (PPU), and a simple propellant flow control system. The first implementation of this technology was a laboratory model (LM) thruster known as the H64M-LM [5] [6]. The H64M-LM demonstrated that a sub-kW magnetically optimized Hall-effect thruster with center mounted cathode can produce adequate performance for high delta-v NASA deep space missions. The H64M-LM requirements were based on NASA internal mission trades and preliminary inputs from U.S. industry partners. Once the H64M-LM demonstrated the propulsion system's feasibility to meet those requirements, the SSEP project sought a more involved working relationship with U.S. industry to further mature the system requirements and produce a pathfinder model (PM) thruster.

The pathfinder propulsion system design incorporates many flight-like features, while retaining much of the flexibility of a laboratory model system. For example, the thrust producing end of the H71M-PM thruster was developed as flight-like as deemed practical, while the upstream interfaces remained rudimentary, allowing easy disassembly, modification, and inspection. The high-level requirements for the H64M-LM and H71M-PM are provided in Table 1. Side by side images of the H64M-LM and H71M-PM are provided in Fig. 1. The propulsion system power level, propellant throughput, lifetime, on/off cycles, voltage range, and performance requirements all increased between the H64M-LM and H71M-PM. These requirement changes were motivated to encompass the requirements of numerous NASA and commercial mission concepts reviewed.

The SSEP project continues to mature a 1-kW PPU to compliment the thruster maturation. The first generation of the PPU power supplies has previously been reported [5] and demonstrated through a successful integrated system test. A second generation of the PPU power supplies has been designed and manufactured. The second generation reflects the H71M-PM operating requirements and furthermore matures packaging, circuitry, and capabilities for telemetry. The magnet, cathode heater, keeper, and ignitor power supplies have each been bench tested. The heater, keeper, and ignitor have been recently demonstrated in an integrated test with an operational cathode. An integrated system test of all second-generation power supplies with the H71M-PM is planned.

Data gathered with the pathfinder propulsion system are supporting design of the H71M-EM engineering model thruster. The H71M-EM makes incremental improvements to the thrust producing end of the thruster and matures the

Table 1. SSEP H64M and H71M high-level propulsion system requirements.

Parameter	Units	H64M	H71M
Total Propellant Throughput	kg	> 90	> 140
Total Impulse	MN-s	> 1	> 2.5
Lifetime	hours	> 10,000	> 14,000
On / Off	Cycles	> 5,000	> 8,000
Thruster Power Range	W	200 - 600	200 – 1,000
Thruster Voltage Range	V	200 - 300	200 - 400
Thrust Capability	mN	> 32	> 50
Specific Impulse Capability	s	> 1500	> 1700
Thruster Efficiency Capability	%	> 50	> 50
Thruster Mass	kg	< 2.5	< 3.5
PPU Input Voltage	V	24 – 34	24 - 34

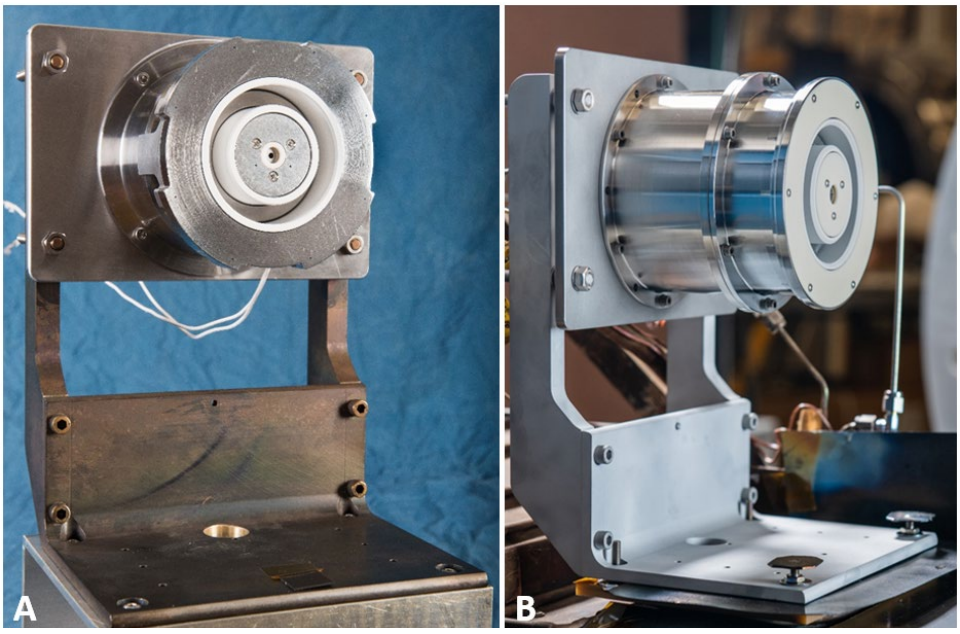

Fig. 1. (Left) NASA H64M-LM Hall-effect thruster and **(Right)** NASA H71M-PM Hall-effect thruster mounted on thrust stand adapter brackets prior to their first operational tests in a vacuum environment.

mechanical, thermal, propellant, and electrical interfaces to the spacecraft.

IV. Thruster Characterization

The H71M-PM has demonstrated stable operation between 200 W and 1 kW. The most recent performance data collected is shown in Fig. 2, although the lowest power operating conditions were not captured during this recent performance characterization. The calculation of specific impulse includes both anode and cathode propellant flows. Thruster efficiency includes discharge and magnet power. Thrust data has an uncertainty of about ± 1% of the measurement, while specific impulse has an uncertainty of about ± 1.5% of the calculated value. Discharge voltage and current are measured to better than ± 100 mV and ± 5 mA, respectively.

Thruster characterization occurred in Glenn Research Center's Vacuum Facility 8 (VF8). The VF8 facility is a 1.5-m diameter, 4.5-m long chamber whose pumping train (including four cryo pumps) can achieve a no-load base pressure of about $1x10^{-7}$ Torr-N_2. A null-style, inverted-pendulum thrust stand of heritage GRC design was installed in VF-8 and tuned for low-thrust measurements. The facility pressure during thruster operation was roughly $1x10^{-5}$ Torr-Xe (flow rate dependent) as measured at the facility walls using two Granville-Phillips 392 vacuum gauges.

The H71M-PM thruster has completed multiple characterization tests. Thruster aging was simulated to assess both beginning of life (BOL) and end of life (EOL) performance by making incremental hardware modifications simulating accelerated erosion. The BOL data will not be presented here as it does not reflect a lifetime average performance. The EOL conditions were achieved by performing two 500-h short duration wear tests (SDWT). The discharge chamber exit ring was incrementally machined for each of the SDWTs to progressively achieve the anticipated EOL profile. In each case, the machined profiles were based on the measured erosion profiles of the prior SDWT and compared against data generated with numerical modeling tools. The third SDWT was performed to validate that EOL the condition was in fact achieved following the first two SDWTs. The data shown in Fig. 2 was collected following the second SDWT. A subset of these performance conditions was verified following the third SDWT to confirm consistent performance. Time dependent thrust and specific impulse data collected during the third SDWT at 800 W and 350 V is presented as Fig. 10, which illustrates the stability of performance. It should be noted that the "EOL condition" should not be interpreted to mean a thruster configuration without further life, rather a thruster configuration that has achieved a sufficiently low rate of discharge channel and pole cover erosion to achieve stable performance for the remainder of the thruster's lifetime. Of the target 14 kh lifetime, the EOL condition will likely be achieved within the first couple thousand hours. The data presented in Fig. 2 is believed representative of mission lifetime average performance, although the data has not been corrected for facility effects to determine in-space performance. Vacuum facility performance data should be corrected before using for mission analyses. The

SSEP project is presently collecting data necessary to correct the test facility performance data for in-flight operations.

The H71M thruster has demonstrated a thrust as high as 68 mN at 300 V and 1 kW of discharge power as measured in the ground test facility. The thruster has similarly demonstrated a specific impulse of 1850 s at 400 V and 1 kW. The thruster operation is stable over the full 200 W to 1 kW operating range, although the thruster may not operate stably at higher voltages at lower power conditions. As shown in Fig. 2D, Hall thruster efficiency is strongly driven by discharge current. For a given power, increasing voltage reduces discharge current. Lower discharge current results in reduced propellant ionization and can lead to thruster instabilities. However, these regions of operational instability are easily identified and avoided. Furthermore, because lower thruster efficiency occurs at lower discharge currents, peak specific impulse does not necessarily occur at peak voltages. So, higher voltage operation at lower power is typically not desirable. Selection of mission operating conditions is mission specific and will depend on a spacecraft's power limitations, delta-v requirement, mission duration, and other mission specific parameters. The data presented in Fig. 2 envelope the H71M performance based on the generalized requirements under which it was developed.

Performance data was further gathered as a function of magnetic field strength between about 0.75x and 1.25x of the nominal value. This data is presented in Fig. 3. Data was collected for several conditions from 250 V to 400 V and

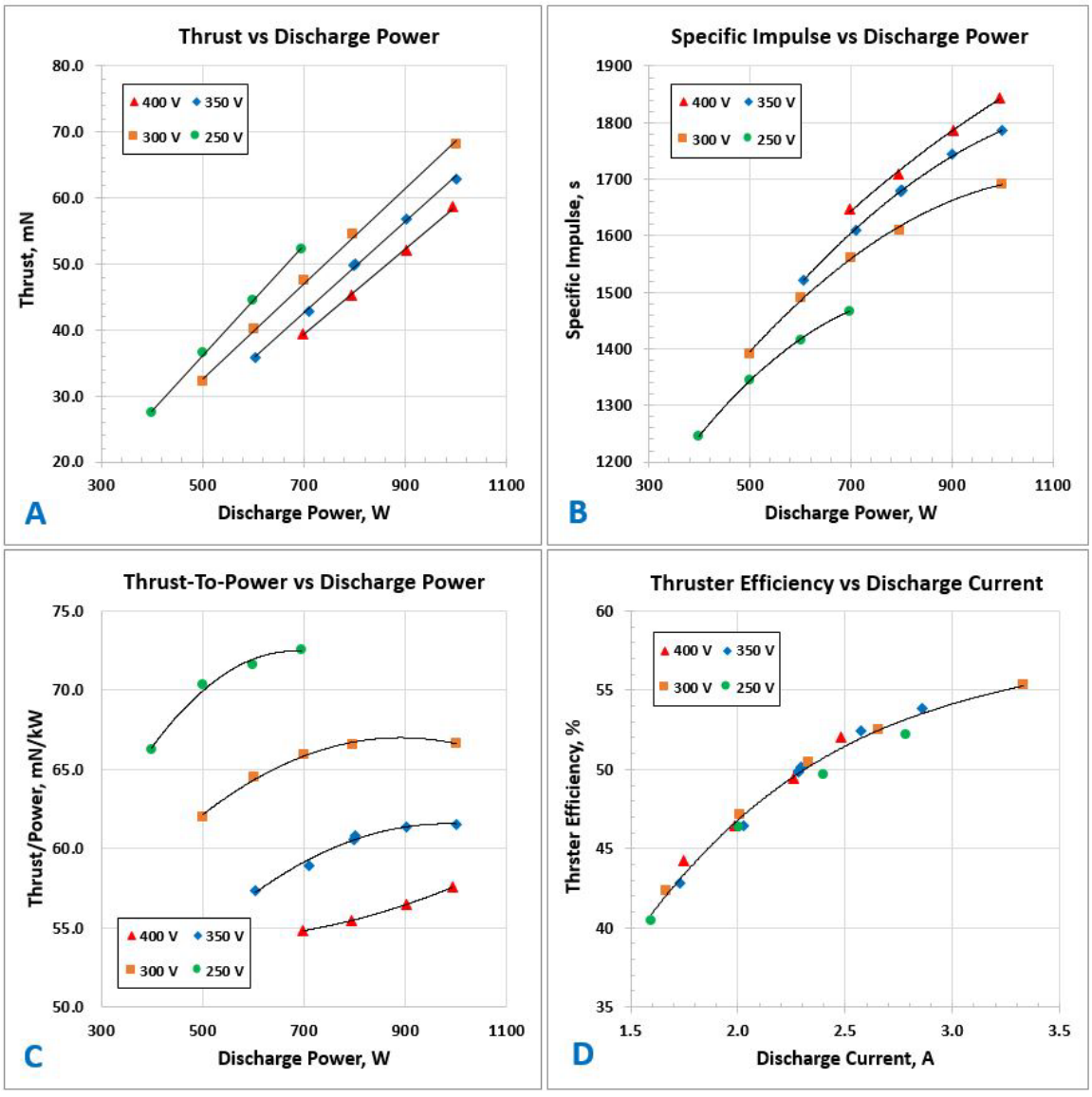

Fig. 2. H71M-PM thruster performance data collected following the 2nd SDWT. **(A)** Thrust as a function of discharge power. **(B)** Specific impulse as a function of discharge power. **(C)** Thrust-to-Power as a function of discharge power. **(D)** Thruster efficiency as a function of discharge current.

600 W to 1 kW. Plots include both thrust-to-power and amplitude of discharge current oscillations as a function of centerline magnetic field strength. The magnetic field strength is set by varying current to the thruster's coils and knowledge of the thruster's magnetic circuit design. Magnetic field strength is not directly measured during thruster operation, although it was confirmed during thruster fabrication. The H71M-PM demonstrates generous magnetic field strength margin across the operational envelope.

The H71M thruster has been observed to operate in one of four modes, Fig. 4: (1) a quiescent mode, where the peak-peak current oscillation is approximately 20% of the mean dc current, (2) a dynamic mode, where the peak-peak discharge current oscillation is approximately 200% of the mean dc current, (3) mode hopping between the quiescent and dynamic modes, or (4) an unstable mode, identified by a run-away discharge current with severe oscillations.

Thrust for fixed flow rate does not vary drastically over the range of magnetic field strength investigated, however a discernable peak in the thrust-to-power does occur and correlates to the magnetic field strength where the mode transition occurs. Thruster performance is generally best in the quiescent mode and operating near the transition point. As transition to the dynamic mode occurs, thrust-to-power drops noticeably, although not especially well exemplified by the data set in Fig. 3 since in this instance data was not collected at higher magnetic field strengths than the bare onset of the mode transition. Roughly speaking, the H71M-PM operates with about a 2-5% reduction in thrust-to-

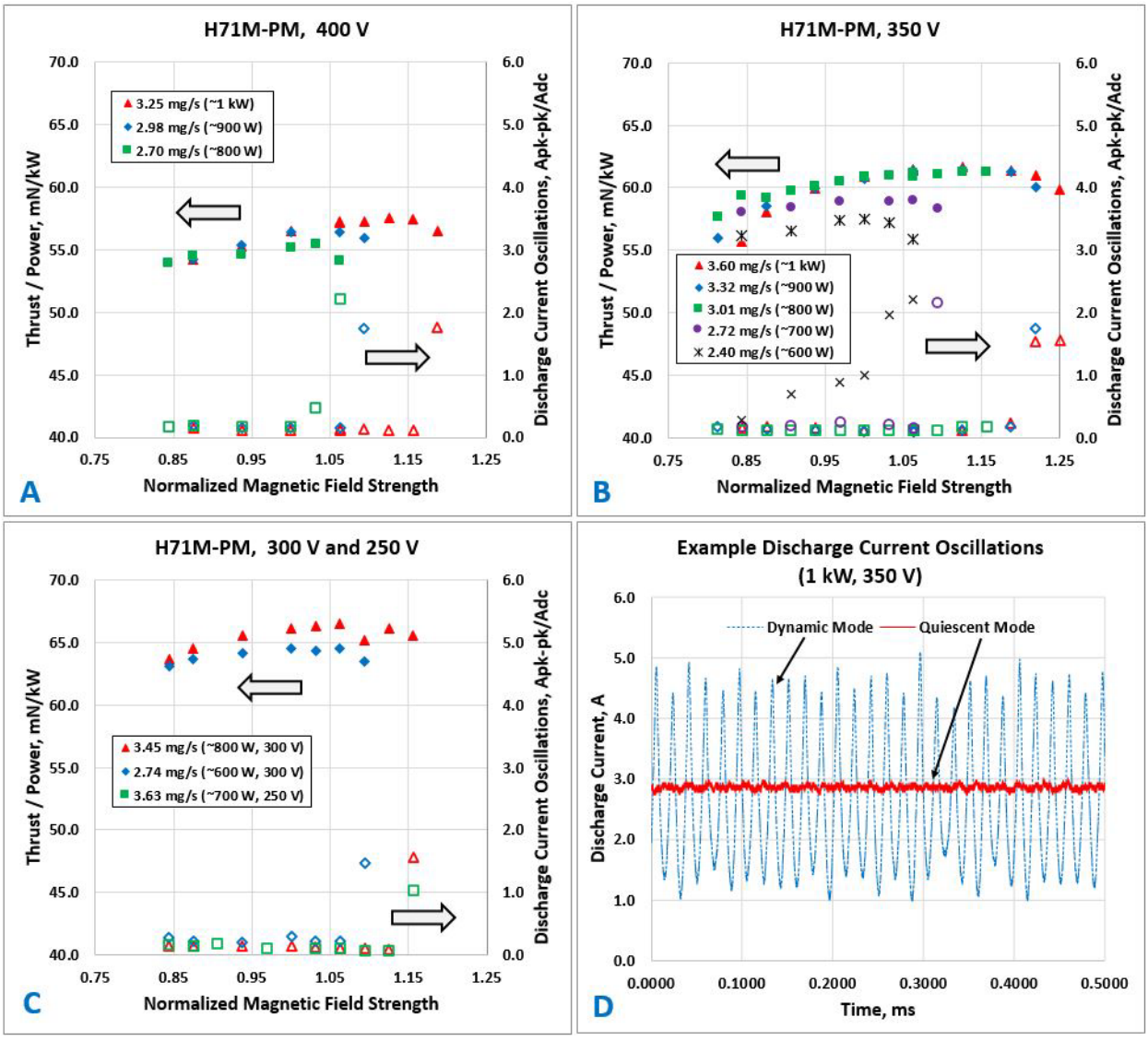

Fig. 3. Thrust-to-Power and amplitude of discharge current oscillation as a function of magnetic field strength. **(A)** 400 V data, **(B)** 350 V data, **(C)** 300 V and 250 V data, **(D)** example discharge current oscillations. Solid markers are thrust-to-power, while open markers of the same shape are discharge current oscillations at the same condition.

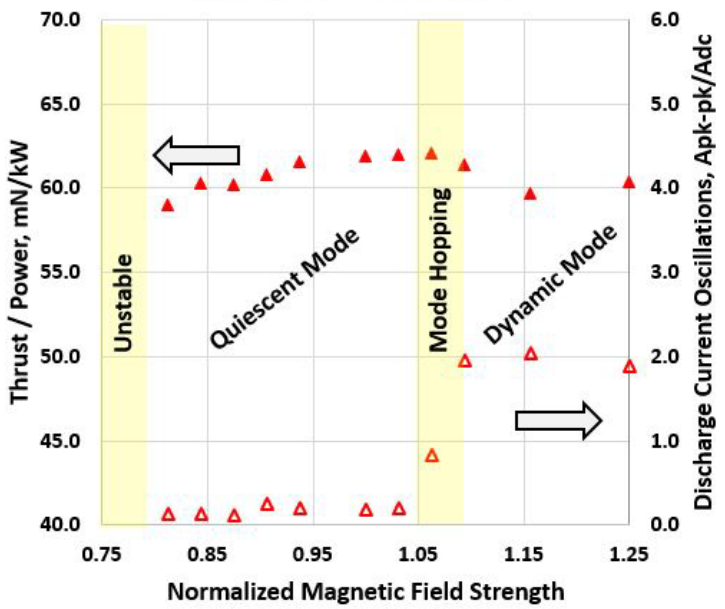

Fig. 4. H71M operating modes example. Modes include (1) Quiescent, (2) Dynamic, (3) Mode Hopping, and (4) Unstable.

power in the dynamic mode than the quiescent mode. Not only does thrust decrease slightly but discharge current increases in the dynamic mode for the same propellant flow rate, exacerbating the reduction in thrust-to-power. For all test data presented in Fig. 2, data was gathered in the quiescent mode at approximately the optimal coil current, although allowing for adequate margin before the mode transition.

While less efficient than the quiescent mode, the dynamic mode is a stable operating mode. The larger discharge current oscillations should not be mistaken for an instability. The dynamic mode peak-to-peak discharge current oscillation of approximately 200% of the nominal dc value can be acceptable for Hall-effect thruster operation. Unlike an unstable condition, the dc current does not run away. It has further been found that under some circumstances where the H71M-PM could not maintain stable operation in the quiescent mode, the dynamic mode had no such instability. As such, a mission carrying the ability to intentionally switch between the quiescent and dynamic modes of operation by increasing magnetic field strength may have an effective tool to manage certain circumstances where a thruster is otherwise unstable.

Another trend to note from Fig. 3 is that increasing flow rate (i.e., discharge current) for a fixed discharge voltage tends to move the mode transition point to higher magnetic field strength. As such, attempting to operate at higher voltage but lower flow rates limit the range of magnetic field strength where the thruster will reliably remain in the quiescent mode. So, for certain conditions, operating in the dynamic mode may simply be the most practical option. Finally, operating at too low or too high of a magnetic field strength risks falling into an unstable condition with severe discharge current oscillations and run-away dc current.

The observed operating modes of the H71M thruster require further evaluation. Since the quiescent mode may be driven by plasma wall interactions or test facility conditions, the thruster may be sensitive to changes. For example, the location of the mode transition may change with thruster aging or background pressure. If so, the magnetic field strength may need to be adjusted periodically over the thruster's lifetime or in different environments.

V. Subassembly and Component Testing

A. Propellant Flow Azimuthal Uniformity

The H64M and H71M use a novel implementation [9] of a patented NASA propellant distributor (i.e., anode) design [10]. Whereas some prior propellant distributors of this NASA design machine many flow restricting devices directly into a single component within the propellant manifold assembly, the H64M and H71M use individual flow restricting inserts. Although separate flow restricting inserts increase the number of piece parts, and require an integration step such as pressing, screwing, or welding, they also offer numerous benefits. In the absence of insert-style flow restricting devices, a completed propellant distributor assembly must typically be manufactured before flow uniformity can be assessed. Flow restrictor geometries are not easily optically inspected during manufacturing, yet

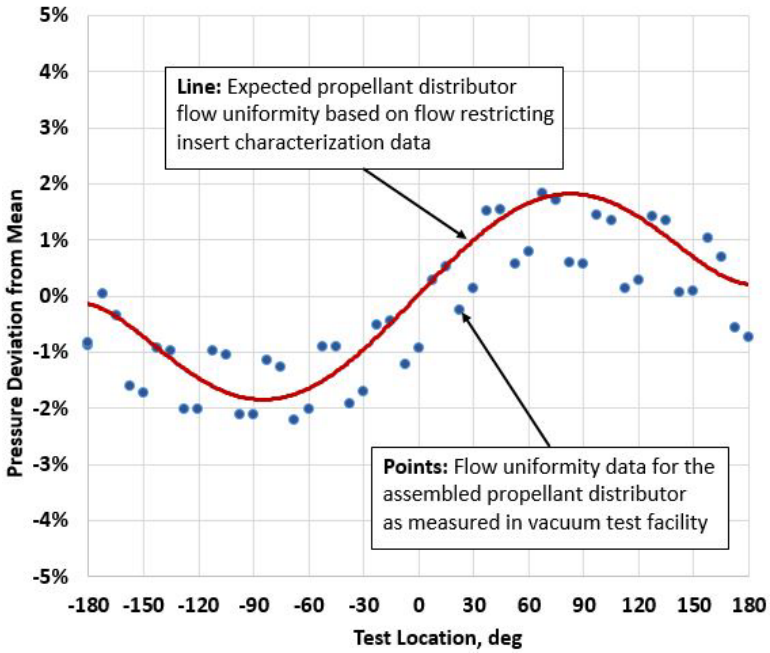

Fig. 5. Azimuthal propellant flow uniformity on thruster centerline at 50% axial distance between the propellant distributor (i.e., anode) face and thruster downstream face.

even minor variations may have a noticeable impact on propellant distributor performance. Good flow uniformity is critical for peak thruster performance and can affect other thruster attributes such as thrust vector alignment, erosion behavior, thermal gradients, and plasma stability. By introducing flow restricting inserts, the flow restrictors can be individually characterized for flow properties and then screened or binned in the manufacturing process with good accuracy. Done well, the risk of scrapping a completed propellant distributor decreases significantly and a costly propellant uniformity test becomes unnecessary.

During fabrication of the H71M-PM flow restrictors were tested and binned based on certain flow properties. The flow restrictors were intentionally arranged to create an easily identifiable sinusoidal pattern and inserted in the anode accordingly. The completed propellant distributor assembly was later tested in a special high vacuum flow uniformity test rig to measure azimuthal flow uniformity, and this data is provided in Fig. 5. The flow uniformity data was measured on the thruster channel centerline at 50% of the axial distance between the propellant distributor face and the thruster downstream face (i.e., approximately in the middle of the discharge channel). The measured azimuthal flow uniformity substantially matches the flow uniformity as predicted by the individual flow restrictor characterization measurements. The scatter in the actual flow uniformity measurement reflects the fact that the propellant injected into the discharge channel has yet to fully diffused at the axial measurement location. While it is not necessarily desirable to intentionally create such a sinusoidal azimuthal non-uniformity in production of a flight thruster, here the flow restrictor insert placement allowed a clear correlation between the insert data and the resulting propellant distributor flow uniformity. A non-uniformity of ± 2% is less than the target flow uniformity for the H71M-PM and is not expected to have a measurable impact on performance measurements presented herein.

B. Magnetic Field Strength Azimuthal Uniformity

During fabrication of the H71M-PM, the thrusters magnetic circuit components were assembled, and the magnetic field strength mapped. While not shown here, the numerical model prediction and the measured magnetic field strength were found to be nearly identical. Fig. 6 shows the magnetic field strength uniformity as a function of discharge channel azimuthal centerline location. The magnetic field strength deviation from the mean centerline value is less than ± 0.5%. Good magnetic field strength uniformity is critical for thruster performance and stability. Measurements made at the nominal and 125% of the nominal magnetic field strength are in good agreement.

C. Cathode Heater Cycle Testing

While high-cycle swaged heaters for cathode applications have been demonstrated repeatedly, the SSEP project

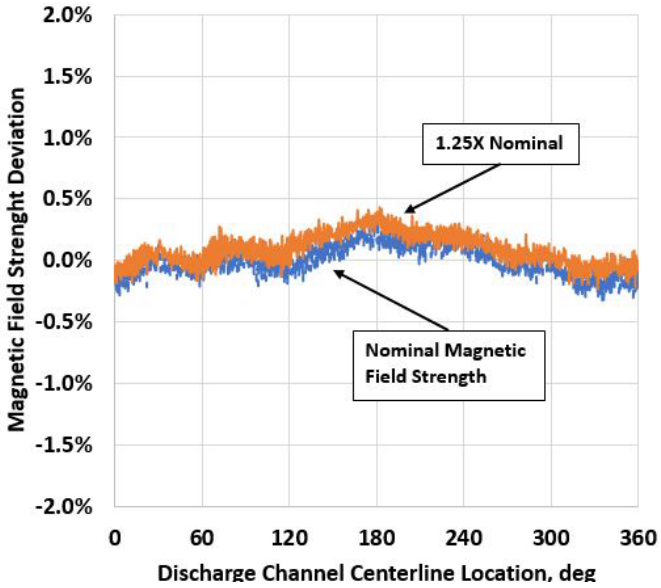

Fig. 6. Azimuthal magnetic field strength deviation relative to the mean value.

seeks to validate the capabilities of commercial sources for smaller diameter swaged heaters as required for the H71M cathodes. Limited NASA experience testing cathode heaters of this size raised concern regarding cycle life relative to the larger devices historically used and understood. Heaters of the required size and materials were obtained from three vendors. Cyclic testing of heaters from one of these vendors (referred to as Vendor 2) is reported on here. Testing of heaters from the remaining two vendors has not yet been completed.

To expediently demonstrate heater cycling lifetime, an accelerated operating profile previously developed was employed to enable comparison of cathode operational behavior [11]. While the SSEP cathode is a smaller device than prior heaters used, the temperature critical elements of the hollow cathode have remained the same along with the hollow cathode ignition procedure. These factors continue to drive the required heater operating time for each cathode ignition and serve as the basis for heater component testing. Consequently, the cyclic on/off profile consisted of a 6-minute powered stage and a 4-minute unpowered stage. The 'on' time duration is based on the discharge ignition

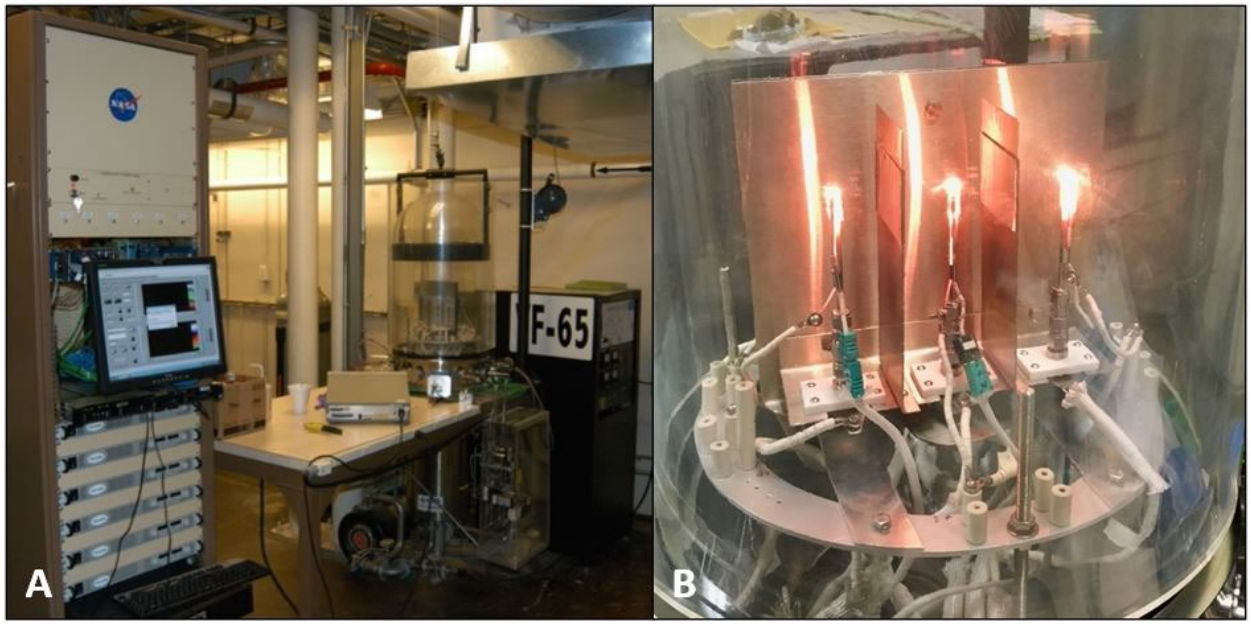

Fig. 7. (A) Cathode Heater Life Test Stand, **(B)** Cathode heaters powered during cycle testing.

procedure and represents the nominal powered period for typical cathode start-up. The 'off' time is the accelerated part of the cycle and captures much of the cool-down of the cathode and subsequently most of the temperature change that the cathode and heater will experience.

A dedicated cathode heater cycle test stand, shown in Fig. 7A, has been used to verify heater capability for multiple projects. When the heater is 'on', it is powered at a constant current that was experimentally determined on representative hollow cathodes. Heater electrical performance is monitored during the powered stage. Type-R thermocouples are attached to refractory metal tubes that serve as cathode tube analogs during this testing. The heater test configuration in the test facility is shown in Fig. 7B where three heaters are shown in the powered condition.

Prior to life testing, the heaters were confidence tested to determine the viability of each heater unit for life testing. The acceptance criterion used in this phase is the change in hot resistance at the end of the 'on' phase that occurs in each heater during the first 150 cycles. Further detail on the heater testing configuration, facility, and confidence testing procedure are provided elsewhere [12] [13].

The heater performance was monitored by tracking the heater power and hot resistance based on the heater voltage and current measured at the end of each powered cycle. Two batches of heaters were procured and tested from Vendor 2. Fig. 8A shows the normalized heater power vs cycle number for Vendor 2, Batch 1, while Fig. 8B shows the same behavior for Vendor 2, Batch 2. Heater failures in Fig. 8A are indicated by the instantaneous drop in heater power.

The total number of accumulated cycles and failure behavior is summarized in Table 2. Failures occurred either with the heater going open circuit suggesting a physical break in the heater element, or the heater 'shorted' at some point along the electrical path which resulted in the heater voltage to drop suddenly. Some of the heaters continued to run stably after experiencing a relatively small voltage drop (~1 V) so they continued to be cycled until a more significant voltage change or open circuit failure was observed.

Table 2. Cathode heater failure summary.

Heater ID	Accumulated Cycles	Failure Mode
V2 - H1-1	14725	Open
V2 - H1-2	25060	Short/Open
V2 - H1-3	33570	Short/Open
V2 - H2-1	33560	Suspended
V2 - H2-2		
V2 - H2-3		

None of the batch 2 heaters failed prior to the test being voluntarily suspended at 33,560 cycles. It is unclear why the batch 2 heaters have demonstrated better cycle life than batch 1. Both heater batches were procured to nearly the

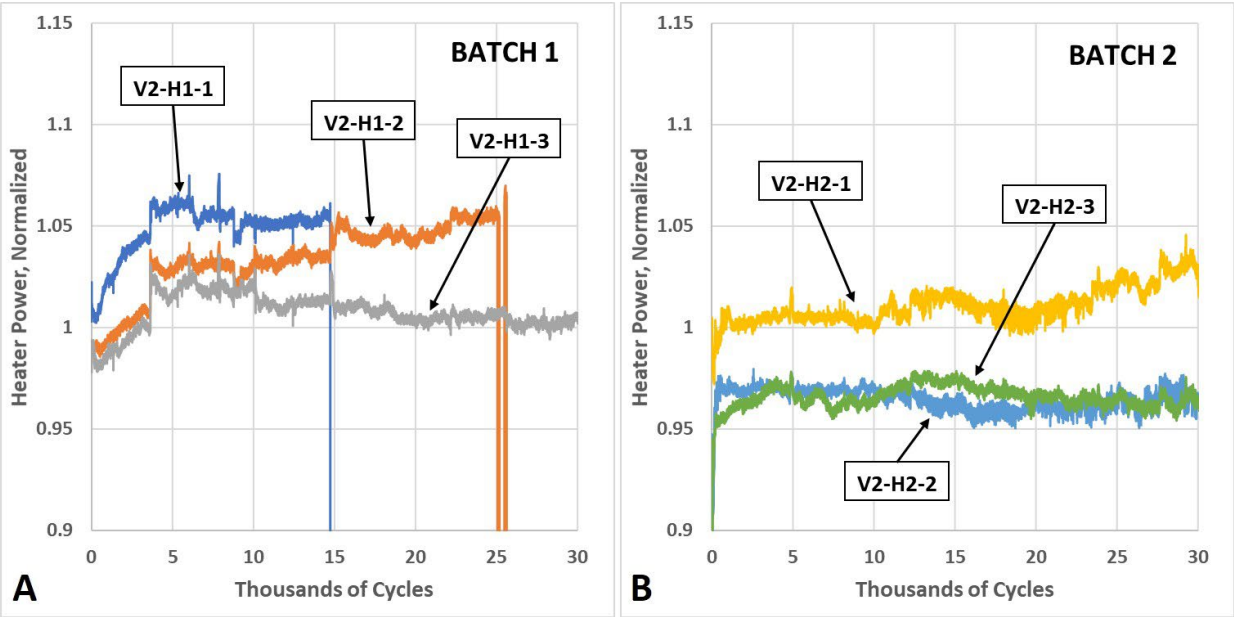

Fig. 8. Heater power (normalized) vs. accumulated cycles for Vendor 1, (A) batch 1 units, (B) batch 2 units.

same specification. Possibilities for the differences in cycle life could be variation in the manufacturer's processes or how the cathode heaters were handled at GRC and installed on the test rig. Insufficient data presently exists to identify the root cause. Although heater cycle life varied considerably across both batch 1 and 2, all heaters exceeded the 8,000-cycle target capability with greater than 50% margin.

VI. Thruster Lifetime Assessment through Accelerated Lifetime Testing

The SSEP project performed three SDWTs of approximately 500-hr duration at 800 W, 350 V to measure pole cover and discharge channel erosion to assess thruster lifetime driven by the degradation of these critical components. The discharge power and voltage were selected based on feedback from stakeholders for near term mission applications. Future testing will be required to further evaluate wear rates at flight specific operating conditions.

Before each test, the pole covers were hand polished and scanned in a Zygo optical profilometer. Polishing removes the machining patterns not visible to the naked eye yet interfere with masked erosion measurements of small steps. Three masks were applied to both the inner front pole cover (IFPC) and outer front pole cover (OFPC) as shown in Fig. 9. Following approximately 500 hours of operation in VF8, the pole covers were removed and again scanned in the Zygo optical profilometer. Wear rates of the pole cover surface were computed by analyzing the steps created around the masked regions. All OFPC mask profiles were successfully evaluated following the methods of NASA-TM-2020-220339.

Each of the first two SDWTs provided insight into the BOL evolution of the discharge channel and pole cover surfaces. Following the first and second SDWTs, the discharge channel and pole covers were incrementally modified to approach the EOL configuration. The goal of the third SDWT was to measure erosion rates in the established EOL condition. However, erosion of the inner and outer pole cover corners during the early phase of the third SDWT likely reduced the average rate of erosion of the pole cover faces. The IFPC and OFPC had been modified with chamfers prior to the third SDWT to eliminate pole cover corner erosion from reducing the average rate of erosion of the pole cover faces. However, while the discharge channel leading edge showed little evidence of significant further erosion as desired, the corners of the pole covers were seemingly insufficiently chamfered to properly reflect EOL.

Following the third SDWT, the erosion rates determined from the three OFPC masked regions were consistent and indicated a maximum rate of erosion of 40 micrometer per kilohour, although concern exists whether insufficient chamfering of the pole covers may have impacted the result. Nonetheless, this result of 40 micrometer per kilohour is likely a reliable lower bound for the OFPC wear rate. The IFPC wear measurements from this test were less than the OFPC, but similarly not conclusive. Future testing will repeat these erosion measurements to better bound the erosion rates. The backsputter rate from the vacuum test facility was successfully estimated through analysis of witness samples to be on the order of 2 micrometers per kilohour and thus a negligible impact on the erosion measurements.

While the third SDWT profilometry erosion measurements are not by themselves conclusive, coupled with other data such as pole cover mass loss, the data does indicate that 14 kh of thruster operation with 50% margin is highly feasible with the current design. Given the pole cover initial thicknesses, the measured wear rate can increase by nearly a factor of two and the lifetime target of 14 kh with 50% margin will remain achievable.

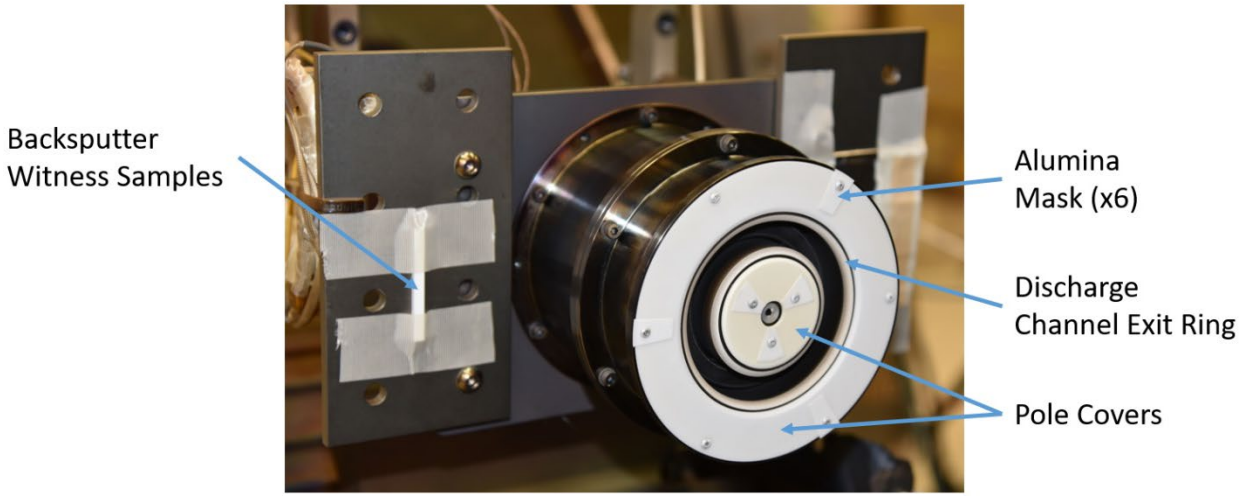

Fig. 9. H71M-PM as configured for the third SDWT.

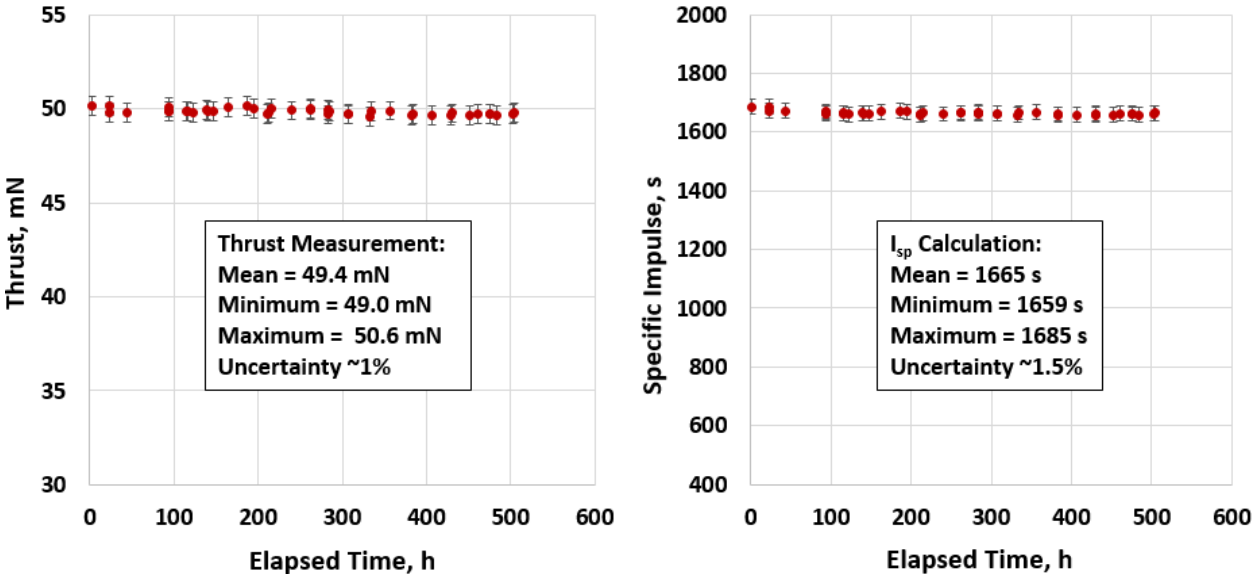

Fig. 10. Performance data collected during the H71M-PM third SDWT, **(Left)** thrust as a funciton of elapsed test time, **(Right)** specific impulse as a function of elapsed test time.

Thrust data was collected throughout the third SDWT at 800 W, 350 V and is presented in Fig. 10. Within the uncertainty of the measurement, both the measured thrust and calculated specific impulse are flat. This is a good indication that the thruster was in fact in a nearly EOL configuration, where discharge channel and pole cover erosion rates have substantially slowed and the performance will remain largely unchanged for the remainder of the thruster's life.

Acknowledgments

Numerous NASA GRC civil servants and contractors have supported the SSEP work described in this paper. The authors would like to thank Tim Smith and Eric Pencil for project management; David Jacobson for technical leadership; Mike Mcvetta for test facility management; Mike Depauw, Rich Senyitko, Nick Lalli, and Sandra Doehne for test facility leadership; Randy Clapper for design support; Ariel Dimston for structural engineering support; Jim Myers for thermal modeling support; Kevin Blake and Josh Gibson for thruster assembly support; Mike Arnett, James Sadey, and Zach Buchman for test facility engineering support; Tom Ralys and Matt Daugherty for test facility equipment fabrication and test preparation. The authors would also like to thank Carolyn Mercer and Brian Smith for their unwavering support of the SSEP project's goals. The SSEP project has been jointly sponsored by NASA's Space Operations Mission Directorate, Space Technology Mission Directorate, and the Science Mission Directorate.

References

[1] NASA, "NASA 2018 Strategic Plan," NASA Headquarters, 2018.
[2] NASA, "NASA State-of-the-art Small Spacecraft Technology Report," NASA/TP-20210021263.
[3] "MarCO", eoPortal Directory, URL: https://directory.eoportal.org/web/eoportal/satellite-missions/content/-/article/marco
[4] Ziemer, J. K., Marrese-Reading, C. M., Arestie, S. M., Conroy, D. G., Leifer, S. D., Demmons, N. R., Gamero-Castano, M., and Wirz, R. E., "LISA Colloid Microthruster Technology Development Plan and Progress," 36th IEPC, Vienna, Austria, 2019.
[5] Benavides, G. F., Kamhawi, H., Liu, T. M., Pinero, L. R., Verhey, T. R., Rhodes, C. R., Yim, J. T., Mackey, J. A., Gray, T. G., Butler-Craig, N. I., Myers, J. L., and Birchenough, A. G., "Development of a High-Propellant Throughput Small Spacecraft Electric Propulsion System to Enable Lower Cost NASA Science Missions," NASA/TM-2019-220330.
[6] Kamhawi, H., Liu, T. M., Benavides, G. F., Mackey, J. A., Server-Verhey, T., Yim, J., Butler-Craig, N. I., and Myers, J., "Performance, Stability, and Thermal Characterization of a Sub-Kilowatt Hall Thruster" 36th International Electric Propulsion Conference, University of Vienna, Austria, Sept. 15-20, 2019, IEPC-2019-910.
[7] NASA, "Small Spacecraft Electric Propulsion (SSEP) Technology Suite (LEW-TOPS-162)," URL: https://technology.nasa.gov/patent/LEW-TOPS-162
[8] NASA Announcement of Opportunity, "Small Innovative Missions for Planetary Exploration," NNH17ZDA004O-SIMPLEX, Released March 22, 2017.

[9] NASA, “Anode Manifold Plug for Hall Effect Thrusters (LEW-TOPS-159),” URL: https://technology.nasa.gov/patent/LEW-TOPS-159
[10] Huang, W. and Yim, J., “Propellant distributor for a thruster,” US 10,273,944 B1, April 30, 2019.
[11] Mueller, L.A., “High Reliability Cathode Heaters for Ion Thrusters,” AIAA International Electric Propulsion Conference, Key Biscayne, FL, Nov. 14-17, 1976.
[12] Verhey, T.R., Soulas, G.C., and Mackey, J.A., ‘Heater Validation for the NEXT-C Hollow Cathodes,’ IEPC-2017-397, 35th International Electric Propulsion Conference, Atlanta, GA, Oct. 2017.
[13] Arthur, N.A. et al. “Qualification of the Flight Heaters for the NEXT-C Hollow Cathodes,” AIAA-2019-4167, AIAA Propulsion & Energy Forum, Indianapolis, IN, Aug. 19-22, 2019.